

**EUROPEAN ORGANIZATION FOR NUCLEAR RESEARCH  
ORGANISATION EUROPEENNE POUR LA RECHERCHE NUCLEAIRE**

**CERN - PS DIVISION**

PS/ PA/ Note 93-28

**INITIAL TESTING OF SEPTUM SMH 58 (LEAD ION)**

J. Borburgh, M. Hourican

Geneva, Switzerland  
30 November, 1993

PS / PA/ Note 93-28  
30 november 1993

## **INITIAL TESTING OF SEPTUM SMH 58 (LEAD ION)**

**J. Borburgh, M. Hourican**

## Contents

1. Introduction
  2. Inductance measurements
  3. Magnetic measurements
    - 3.1 Measurements inside the magnet gap
    - 3.2 Measurement of the stray field next to the septum
    - 3.3 Measurement of the leakage field at the magnet ends
  4. Current wave form measurements
  5. Conclusions
- 
- Appendix 1. Comparison between old and new SMH58 magnets
  - Appendix 2. Magnet characteristics for lepton operation at 3.5 GeV/c, deflection 19 mrad
  - Appendix 3. Magnet characteristics for lepton operation at 3.5 GeV/c, deflection 25 mrad
  - Appendix 4. Magnet characteristics for proton operation at 10 GeV/c, deflection 25 mrad
  - Appendix 5. Magnet characteristics for proton operation at 12 GeV/c, deflection 25 mrad

## 1. Introduction

Before installation in the PS complex it was necessary to test the magnets at various currents corresponding to the various beam energies required. Tests were carried out to assess the cooling system, to perform magnetic measurements and compare with the calculated design values and to examine the current wave form when pulsed at different current levels. The results of these tests are tabulated in this report.

Figure 1 shows the circuit diagram is shown and the place where induction measurements were made. In figure 2 the positions are indicated where the different magnetic measurements were taken.

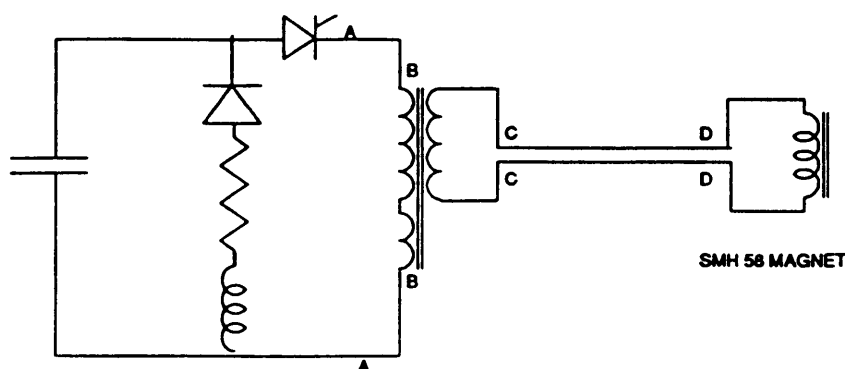


Figure 1: the circuit diagram

The circuit specifications were:

Capacitance	2 mF
Transformer	12 : 1

The measuring equipment used was:

Impedance meter	H.P. Model
Current Transformer	Pearson Model 1423 (1 V/kA)
Digitiser	Tektronix 7612D
Oscilloscope (Bdl measurements)	Tektronix 7854
Data handling	Tektronix 4052A
Scope	H.P. Model 54601 A

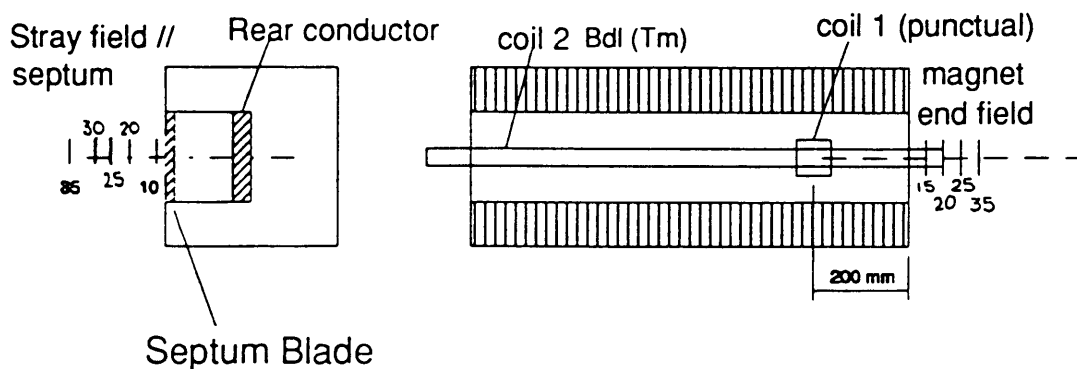


Figure 2: magnetic measurement positions

## 2. Inductance measurements

Using an impedance meter the individual values of resistance and inductance of each component in the discharge circuit were measured at two frequencies. By bridging the circuit at various points the inductance as seen by the primary of the power supply can be determined. In table 1 the results are reproduced. The short circuit points are indicated in figure 1.

Table 1 : inductance measurements

Frequency	SMH 58 (old)		SMH 58 (2)IPb		SMH 58 (1)IPb	
	1 kHz	120Hz	1 kHz	120Hz	1 kHz	120Hz
Inductance	L( $\mu$ H)	L( $\mu$ H)	L( $\mu$ H)	L( $\mu$ H)	L( $\mu$ H)	L( $\mu$ H)
Short circuit @						
B	13		13.1	15	13	14
C	60		59.7	67	58	65
D	94.1	112	98	110	98.1	109
No short circuit	558	582	453	479	452	479
Calculated Real magnet inductance	3.22	3.26	2.46	2.56	2.45	2.56

The inductance values for magnets SMH58.1 and SMH58.2 do not differ much from each other, as can be expected. The values measured are within 1% of the values calculated. The inductance of these new magnets is app. 23% less that the old magnet.

## 3. Magnetic measurements

Using the power supply described previously with a pulse repetition rate of approximately 4.5 seconds a series of measurements were recorded in order to determine the magnetic field in the gap, the stray field close to the septum and the stray field at the magnet ends. The field in the gap was measured to determine the actual punctual values and also the Bdl from which we can calculate the equivalent magnetic length of the magnet. Two types of measuring coils were used and their characteristics are given below.

- a. For punctual field values,

$$\text{Coil 1; surface area} = 0.03693\text{m}^2$$

- b. For Bdl measurements,

$$\text{Coil 2; Surface area} = 0.0750\text{m}^2, \text{ length } 1.303 \text{ m}$$

$$\text{Coil 3; Surface area} = 0.0755\text{m}^2, \text{ length } 1.303 \text{ m}$$

With the small measuring coil (coil 1) the field was measured in the middle of the gap and at  $\frac{1}{4}$  of the length of the septum. With the result the field  $B_0$  in the septum can be calculated for the different currents with the following equation:

$$B_0 = \frac{\int V_{coil} dt}{S_{coil}}$$

With the  $B_0$  known for each current, the equivalent magnetic length of the septum can be calculated i.e. the length of the septum, if in the gap a homogeneous field  $B_0$  existed and outside the field was zero.

The  $L_{eq}$  is calculated as follows:

$$L_{equivalent} = \frac{L_{coil} \int V dt}{S \cdot B_0}$$

The measurements and calculations of these quantities are described in the next paragraphs.

### 3.1 Measurements inside the magnet gap

In this paragraph tables and diagrams are shown of the field in the gap, measured with coil 1, and the integrated field through the gap measured over more than the full length of the magnet to obtain the equivalent length of the magnet. The results for magnet SMH58.2 are shown in tables 2 and 3 and figures 3 and 4.

Table 2:  $B_0$  measurements inside the gap of SMH58.2

Magnet current (A)	$\int V dt$ (Vs) with coil 1	$B_0$ (T)
3600	0.00667	0.181
5420	0.0100	0.271
7150	0.0131	0.356
13130	0.0243	0.658
20430	0.0381	1.03
24516	0.0454	1.23
28764	0.0532	1.44

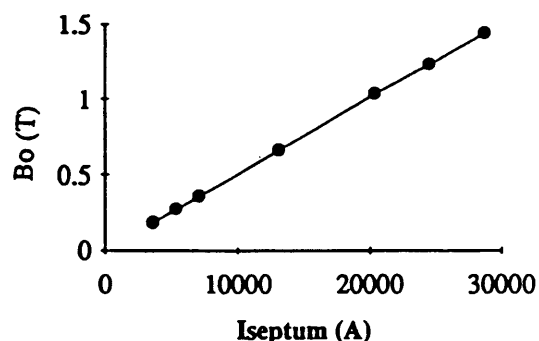


Figure 3:  $B_0$  in the gap of SMH58.2

Table 3: Integrated field measurements inside gap

Magnet current (A)	$\int V dt$ (Vs) with coil 2	$Bdl$ (Tm)
3600	0.00847	0.144
5420	0.0129	0.224
7150	0.0168	0.292
13130	0.0310	0.538
20430	0.0479	0.832
24516	0.0575	0.999
28764	0.0674	1.17

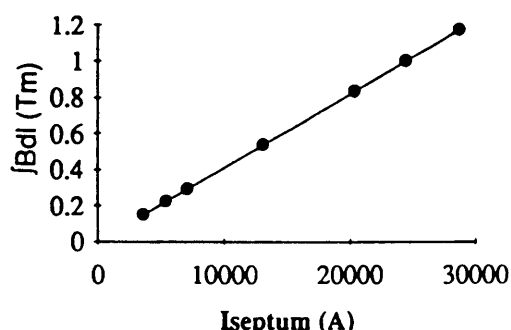


Figure 4:  $Bdl$  measurement in the gap

Two measurements were made with magnet SMH58.1 in order to make a comparison between the two physically identical magnets to ensure that no serious deviations occurred from one magnet to the other.

Table 4: Magnetic measurements inside gap of SMH58.1

Iseptum (A)	$\int V dt$ (Vs) coil2	$\int V dt$ (Vs) coil1	Bdl (Tm)	$B_0$ (T)
5420	0.0128	0.01	0.223	0.27
28764	0.067	0.0526	1.17	1.42

In figure 5 the field  $B_0$  is shown as function of the current through septum magnets SMH58.1 and SMH58.2. What can be noticed is, that no measurable saturation occurs, even for very large currents. Also the differences in field strength is negligible.

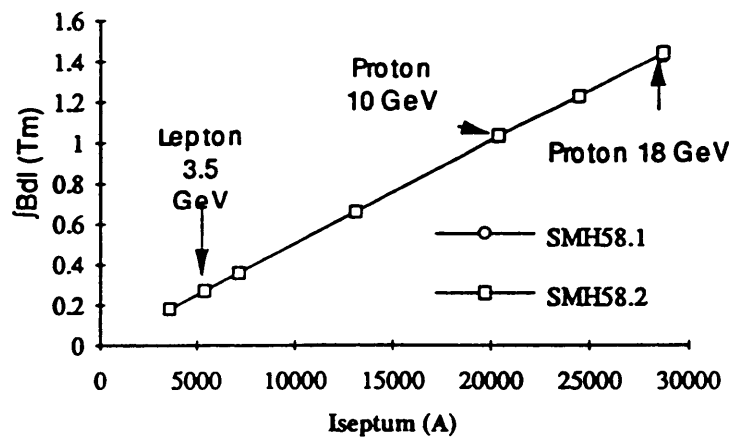


Figure 5: The field inside the septa magnets SMH58.1 and SMH58.2

### 3.2 Measurement of the stray field next to the septum

Measurements were carried out to determine the magnitude of the integrated stray field parallel and close to the septum blade in order to assess the effect on the orbiting beam. The results were taken at five separate distances from the septum with results presented in table 5a and 5b.

With the third coil, coil3, the integrated field (Bdl) was measured for magnets SMH58old and SMH58.2. With coil1 the specific field strength was measured for magnet SMH58.2. The results are shown in the table 5a and 5b. These results are graphically shown in figures 6a and 6b.

Table 5a: Stray field and Bdl measurements on SMH58.2 at I=24516A

Distance from septum blade (mm)	$\int V dt$ (coil3) (mVs)	Bdl (mTm)	$\int V dt$ (coil1) (mVs)	B (mT)
10	0.441			
20	0.191	7.60	0.0780	2.11
25		3.29	0.0564	1.53
30	0.114	1.95	0.0431	1.17
35			0.0320	8.65
40	0.0774	1.33		
50	0.0617	1.06		

Table 5b: Bdl measurements on SMH58old 10 mm from septum

Iseptum (A)	$\int V dt$ (coil3) (mVs)	Bdl (mTm)
5420	0.735	1.27
24520	5.11	8.8
28776	8.81	15.2

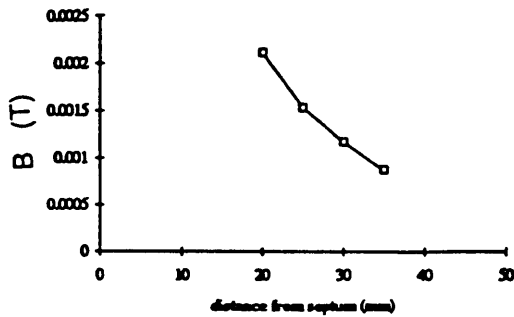


Figure 6a: Punctual stray field next to septum

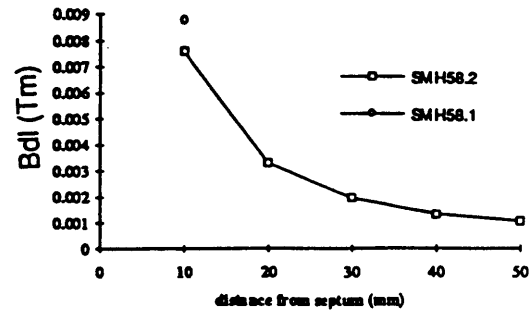


Fig 6b: Integrated stray field parallel to septa

The stray field next to the magnet SMH58.1 is approximately 15% larger than the stray field of magnet SMH58.2. This is due to tolerances in the production of the magnets. The absolute values however of the stray fields are low enough not to affect the circulating beam.

### 3.3 Measurement of the leakage field at the end of the magnet

The field was measured at four positions from the end of the magnet to determine the magnitude of the end field due to leakage. At each of the four positions the current was varied from the lowest value to the highest value.

Table 6: End field for SMH58.2

I magnet (A)	$\int V dt$ (uVs)	B (T)	position (mm)
7128	79.65	2.16E-04	15
7128	53.88	1.46E-04	20
7128	38.99	1.06E-04	25
7128	21.5	5.82E-05	35
20436	305.3	8.27E-04	15
20436	206.2	5.58E-04	20
20436	145	3.93E-04	25
20436	79.2	2.14E-04	35
24516	373.8	1.01E-03	15
24516	257.1	6.96E-04	20
24516	180.3	4.88E-04	25
24516	97.2	2.63E-04	35

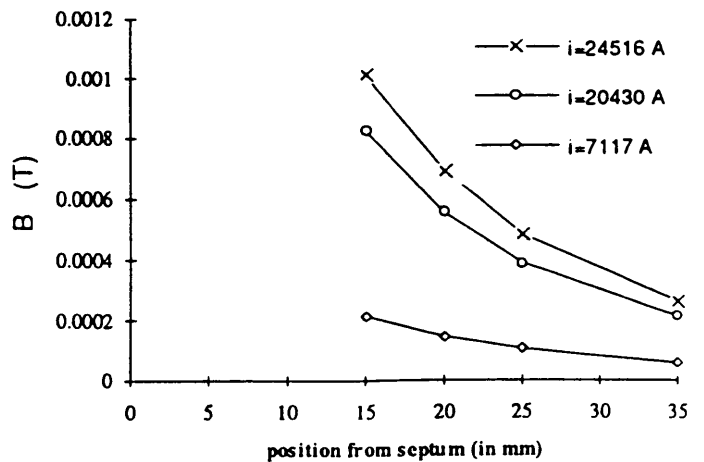


Figure 7: end field at different currents SMH58.2

What can be seen in figure 7 is that the end fields drop very rapidly, as can be expected. This field also contributes to the magnetic length of the magnet. To compare these end fields with theory we calculated from the data of paragraph 3.1 the equivalent



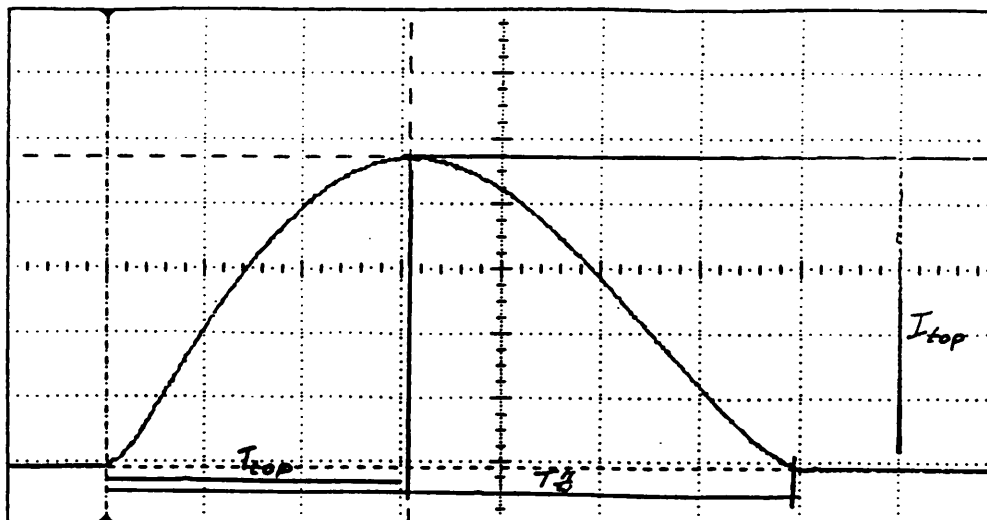


Figure 8: Definition of  $I_{top}$ ,  $T_{\pi/\omega}$  and  $T_{top}$

length of SMH58.2 at different currents. The equivalent magnetic length of a septum magnet that can be expected is the physical length plus half the gap length. The measured length is shown in table 7. What can be seen is that the equivalent magnetic length is within acceptable tolerance limits even though the accuracy of the measurement is relatively low.

table 7: measured and calculated equivalent length of SMH58.2.

Iseptum (A)	3600	5420	7150	13130	20430	24516	28764
Leq. (measured ) (m)	0.813	0.826	0.818	0.816	0.806	0.811	0.812

#### 4. Current Characteristics

The septum magnets were connected to the power supply as shown in figure 1 of this report. The capacitor bank was 2 mF. At different currents the current wave form was measured for magnet SMH58old and SMH58.2. Three characteristic quantities can be defined:

- $I_{top}$ , the top value of the current
- $T_{\pi/\omega}$ , duration of half sine
- $T_{top}$ , time from start until  $I_{top}$  occurs

These quantities are illustrated in figure 8.

In table 8 the values for the defined quantities are shown.

Due to the reduced inductance value of the new series of magnets, we expected a shorter pulse width and this was confirmed by the current signals taken. For SMH58.2 the values for  $T_{\pi/\omega}$  and  $T_{top}$  are 10% and 8% less respectively. The values for these quantities vary approximately 3% for the range of currents that were measured. These variations are in the same order of magnitude as the measurement error. The only conclusion that can be drawn from these measurements is that different currents result in only an small variation in  $T_{\pi/\omega}$  and  $T_{top}$ .

table 8:  $I_{top}$ ,  $T_{\pi/\omega}$  and  $T_{top}$  at different currents for SMH58.1 and SMH58.2

Septum Magnet	$I_{top}$ (kA)	$T_{\pi/\omega}$ (ms)	$T_{top}$ (ms)	Beam momentum (GeV/c)	Deflection angle (mrad)
SMH58old	4.6	3.9	1.7	3.5	19
	7.2	3.85	1.71		
	13.1	3.8	1.65	10	19
	19.4	3.78	1.62		
SMH58.2	7.2	3.5	1.54	3.5	25
	13.1	3.44	1.52		
	20.6	3.4	1.50	10	25

In the figures 9 and 10 the wave forms are shown for SMH58old and SMH58.2.

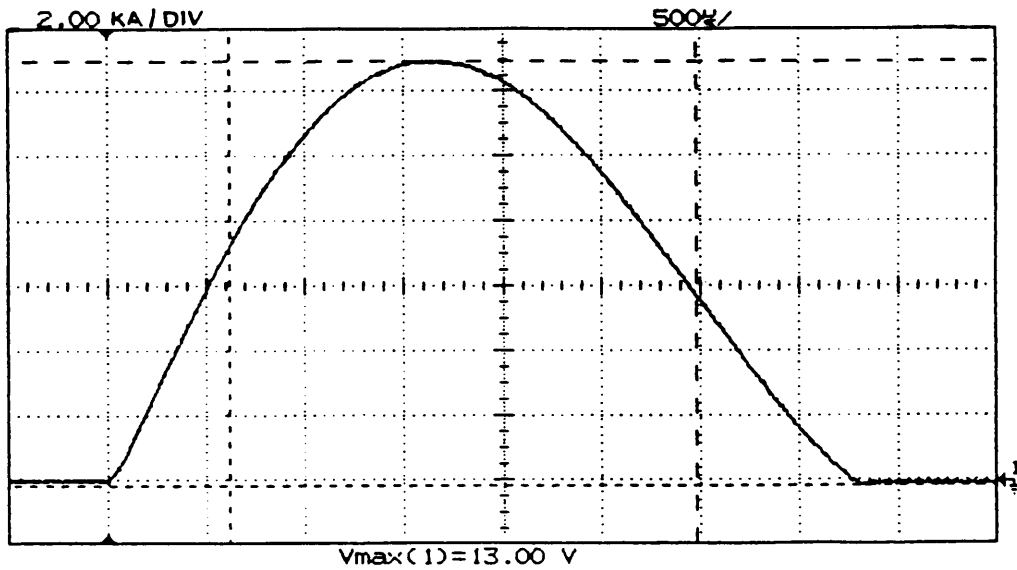


Figure 9: Current wave form SMH58old

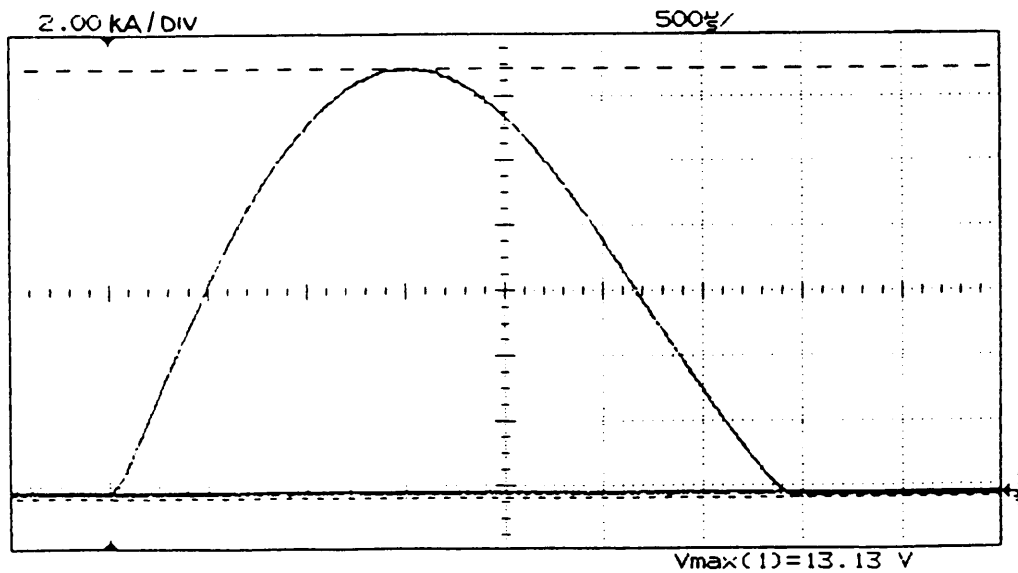


Figure 10: Current wave form SMH58.2

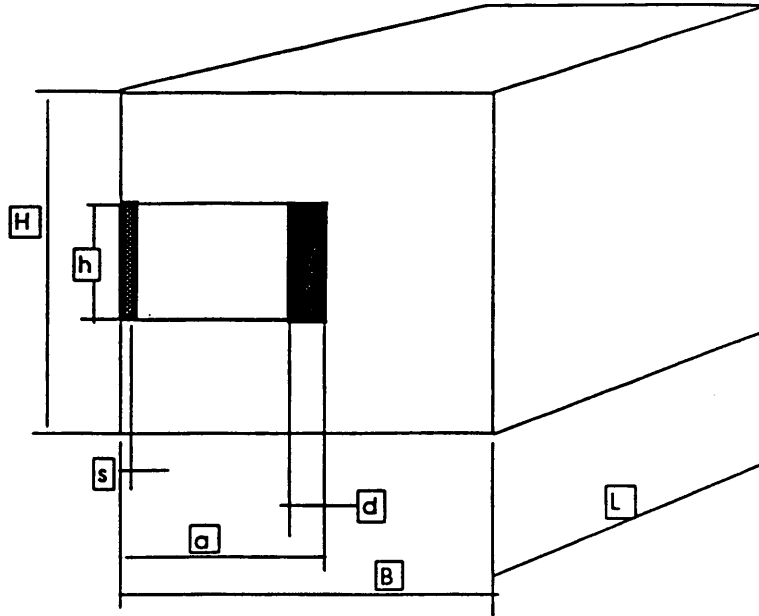
## 5. Conclusions

The inductance measurements have shown that the measured values for the new magnets are within 1% of the calculated ones. This means a reduction of approximately 23% in comparison with the old magnet.

Leakage fields at the ends of the new magnet are as expected, because the equivalent length of the magnet measured is close to the equivalent length expected from the calculations. The stray field next to the septum blade of the new magnets is low, lower than 1% of the gap field at 10mm from the septum, and lower than 1/1000 at 40 mm distance from the septum.

The current wave forms are measured and compared with the current wave forms from the old magnet. Because of the reduced inductance of the new magnets, the pulse width is shorter than the pulse width from the old magnet.

COMPARAISON between OLD and NEW SMH58



all dimensions in mm

	old SMH58	new SMH58
<b>Laminations</b>		
<b>gap</b>		
h	25	25
a	70	65
s	3	3
d	5	6
<b>external</b>		
B	135	140
H	160	140
L total	1020	851
L effective	970	799

**Electrical and magnetic characteristics**

<b>LEPTONS 3.5 GeV/c</b>	<b>deflexion = 19 mrad ( actual deflexion in operation )</b>		
int. B.dl	0.22	0.22	T.m
Bo	0.23	0.27	T
Current	4.5	5.4	kA
<b>ANTIPROTONS 12 GeV/c</b>	<b>deflexion = 19 mrad</b>		
int. B.dl	0.76	0.76	T.m
Bo	0.77	0.94	T
Current	15.4	18.6	kA
<b>ANTIPROTONS 18 GeV/c</b>	<b>deflexion = 19 mrad</b>		
int. B.dl	1.14	1.14	T.m
Bo	1.16	1.4	T
Current	23	28	kA
<b>ANTIPROTONS 26 GeV/c</b>	<b>deflexion = 19 mrad</b>		
int. B.dl	1.65		T.m
Bo	1.68		T
Current	33.3		kA

PREDETERMINATION SEPTUM MAGNETIQUE

SMCALC.XLS

PW prot:MT

type d'aimant

**SMH 58****LEPTONS****3.5 GeV/c**

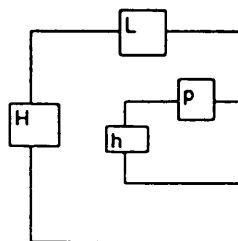
Ions Plomb

DONNEES		
particules electrons : e	protons : p	p
quant.mouv. : MV	Energie cin. : EC	MV
Quantité de mouvement p =	3.5	GeV/c
Déflexion requise	19	mrad
Epaisseur du septum	3	mm
Hauteur du Gap	25	mm
Profondeur du Gap	65	mm
Longueur de la culasse	0.799	m
Espace de glissement	0	m
nombre de spires	1	spire
Hauteur de chaque conducteur	25	mm
Largeur de chaque conducteur	4.5	mm
Résistivité du cuivre ( 1.72E-2	0.0172	mO.mm
module d'Elasticité (12500	12500	daN/mm <sup>2</sup>
Forme de l'impulsion		
DC , 1/2 sinus : S , trapèze : T	S	
1/2 période de l'impulsion	3.4	ms
Période de récurrence (cycle tot. soit le taux de répétition	2.4	s
% du conducteur pour refroidissement	4	%
Elévation de température moy.admise ex: AA avec dT =20 Temp max=60oC	5	oC

## RESULTATS

## PROTONS

Masse au repos m <sub>0</sub>	0.94	GeV/c <sup>2</sup>
Energie cinétique	2.6840	GeV
Quantité de mouvement	3.5000	GeV/c
beta	0.9658	
gamma	3.8554	
beta*gamma	3.7234	
Déplacement sortie septum	7.59	mm
Champ intégré B*L	0.222	T.m
Induction dans le Gap	0.273	T
Champ magn. H=B/uo	2.17E+05	A/m
Courant nécessaire	5434	A
Valeur efficace du courant	145	A
densité de courant eff.	2.41	A/mm <sup>2</sup>
Résistance de l'aimant	0.24	mOhms
Inductance de l'aimant	2.43	uH
Puissance dissipée	0.005	kW
Energie stockée	36	J
	65	p en mm
	25	h en mm
	130	L en mm
	155	H en mm
Débit d'eau total	0.01	l/min
Débit dans chaque spire	0.01	l/min
vitesse de l'eau ( < 10m/s)	0.03	m/s
pression différentielle necess	0.24	bar
Force septum /cond fond	59.30	daN
Flèche max . septum (appui)	0.001	mm
moment flech.max. ( appui)	0.23	mm*daN
contrainte maxi <5 (appui)	0.15	daN/mm <sup>2</sup>
Masse culasse (sans poutre)	106	kg
longueur d'une spire	1.4883	m
section conduct.refroid.déduit	108	mm <sup>2</sup>
Section refroidissement	4.5	mm <sup>2</sup>



PREDETERMINATION SEPTUM MAGNETIQUE

SMCALC.XLS

PW prot:MT

type d'aimant

**SMH 58****LEPTONS****3.5 GeV**

Ions Plomb

DONNEES		
particules electrons : e	protons : p	e
quant.mouv. : MV	Energie cin. : EC	EC
Energie cinétique Ec =	3.5	GeV
Déflexion requise	25	mrad
Epaisseur du septum	3	mm
Hauteur du Gap	25	mm
Profondeur du Gap	65	mm
Longueur de la culasse	0.799	m
Espace de glissement	0	m
nombre de spires	1	spire
Hauteur de chaque conducteur	25	mm
Largeur de chaque conducteur	4.5	mm
Résistivité du cuivre ( 1.72E-2	0.0172	mO.mm
module d'Elasticité (12500	12500	daN/mm2
Forme de l'impulsion		
DC , 1/2 sinus : S , trapèze : T	S	
1/2 période de l'impulsion	3.4	ms
Période de récurrence (cycle tot.	2.4	s
soit le taux de répétition		
% du conducteur pour refroidissement	4	%
Elévation de température moy.admisse	5	oC
ex: AA avec dT =20 Temp.max=60oC		

## RESULTATS

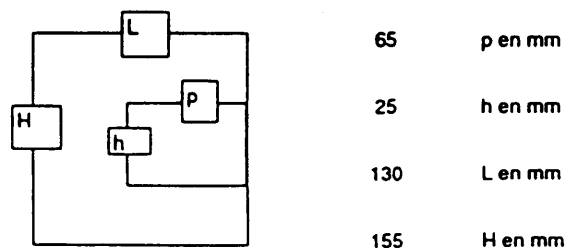
## ELECTRONS

Masse au repos mo	0.000512	GeV/c2
Energie cinétique	3.5000	GeV
Quantité de mouvement	3.5000	GeV/c
beta	1.0000	
gamma	6836.9375	
beta*gamma	6836.9374	

Déplacement sortie septum	9.99	mm
Champ intégré B*L	0.292	T.m
Induction dans le Gap	0.359	T.
Champ magn. H=B/uo	2.86E+05	A/m

Courant nécessaire	7150	A
Valeur efficace du courant	190	A
densité de courant eff.	3.17	A/mm2
Résistance de l'aimant	0.24	mOhms
Inductance de l'aimant	2.43	uH

Puissance dissipée	0.009	kW
Energie stockée	62	J



Débit d'eau total	0.02	l/min
Débit dans chaque spire	0.02	l/min
vitesse de l'eau ( < 10m/s)	0.05	m/s
pression différentielle necess.	0.41	bar

Force septum /cond fond	102.67	daN
Flèche max . septum (appui)	0.001	mm
moment flech.max. ( appui)	0.40	mm*daN
contrainte maxi <5 (appui)	0.27	daN/mm2
Masse culasse (sans poutre)	106	kg

longueur d'une spire	1.4883	m
section conduct. refroid.déduit	108	mm2
Section refroidissement	4.5	mm2

PREDETERMINATION SEPTUM MAGNETIQUE

SMCALC.XLS

PW prot:MT

type d'aimant

**SMH 58****PROTONS****10 GeV/c**

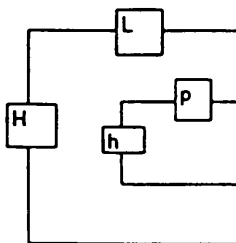
Ions Plomb

DONNEES		
particules electrons : e	protons : p	p
quant.mouv : MV	Energie cin. : EC	MV
Quantité de mouvement p =	10	GeV/c
Déflexion requise	25	mrad
Epaisseur du septum	3	mm
Hauteur du Gap	25	mm
Profondeur du Gap	65	mm
Longueur de la culasse	0.799	m
Espace de glissement	0	m
nombre de spires	1	spire
Hauteur de chaque conducteur	25	mm
Largeur de chaque conducteur	4.5	mm
Résistivité du cuivre ( 1.72E-2	0.0172	mO.mm
module d'Elasticité (12500	12500	daN/mm2
Forme de l'impulsion		
DC , 1/2 sinus : S , trapèze : T	S	
1/2 période de l'impulsion	3.4	ms
Période de récurrence (cycle tot.	2.4	s
soit le taux de répétition		
% du conducteur pour refroidissement	4	%
Elévation de température moy.admise	5	oC
ex: AA avec dT =20 Temp.max=60oC		

## RESULTATS

## PROTONS

Masse au repos mo	0.94	GeV/c <sup>2</sup>
Energie cinétique	9.1041	GeV
Quantité de mouvement	10.0000	GeV/c
beta	0.9956	
gamma	10.6852	
beta*gamma	10.6383	
Déplacement sortie septum	9.99	mm
Champ Intégré B*L	0.833	T.m
Induction dans le Gap	1.027	T
Champ magn. H=B/uo	8.17E+05	A/m
Courant nécessaire	20430	A
Valeur efficace du courant	544	A
densité de courant eff.	9.06	A/mm <sup>2</sup>
Résistance de l'aimant	0.24	mOhms
Inductance de l'aimant	2.43	uH
Puissance dissipée	0.070	kW
Energie stockée	507	J
	65	p en mm
	25	h en mm
	130	L en mm
	155	H en mm
Débit d'eau total	0.16	l/min
Débit dans chaque spire	0.16	l/min
vitesse de l'eau ( < 10m/s)	0.40	m/s
pression différentielle necess.	3.35	bar
Force septum /cond fond	838.12	daN
Flèche max . septum (appui)	0.008	mm
moment flech.max. ( appui)	3.28	mm*daN
contrainte maxi <5 (appui)	2.19	daN/mm <sup>2</sup>
Masse culasse (sans poutre)	106	kg
longueur d'une spire	1.4883	m
section conduct. refroid.déduit	108	mm <sup>2</sup>
Section refroidissement	4.5	mm <sup>2</sup>



PREDETERMINATION SEPTUM MAGNETIQUE

SMCALC.XLS

PW prot:MT

type d'aimant

**SMH 58****PROTONS****12 GeV/c**

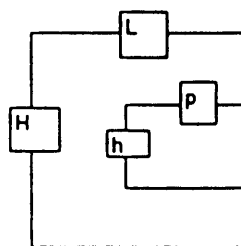
Ions Plomb

DONNEES		
particules electrons : e	protons : p	p
quant.mouv. : MV	Energie cin. : EC	MV
Quantité de mouvement p =	12	GeV/c
Déflexion requise	25	mrad
Epaisseur du septum	3	mm
Hauteur du Gap	25	mm
Profondeur du Gap	65	mm
Longueur de la culasse	0.799	m
Espace de glissement	0	m
nombre de spires	1	spire
Hauteur de chaque conducteur	25	mm
Largeur de chaque conducteur	4.5	mm
Résistivité du cuivre ( 1.72E-2	0.0172	mΩ.mm
module d'Elasticité (12500	12500	daN/mm <sup>2</sup>
Forme de l'impulsion		
DC , 1/2 sinus : S , trapèze : T	S	
1/2 période de l'impulsion	3.4	ms
Période de récurrence (cycle tot.	2.4	s
soit le taux de répétition		
% du conducteur pour refroidissement	4	%
Elévation de température moy.admisse	5	oC
ex: AA avec dT =20 Temp.max=60oC		

## RESULTATS

## PROTONS

Masse au repos m <sub>0</sub>	0.94	GeV/c <sup>2</sup>
Energie cinétique	11.0968	GeV
Quantité de mouvement	12.0000	GeV/c
beta	0.9969	
gamma	12.8051	
beta*gamma	12.7660	
Déplacement sortie septum	9.99	mm
Champ intégré B*L	1.000	T.m
Induction dans le Gap	1.232	T
Champ magn. H=B/μ <sub>0</sub>	9.81E+05	A/m
Courant nécessaire	24516	A
Valeur efficace du courant	652	A
densité de courant eff.	10.87	A/mm <sup>2</sup>
Résistance de l'aimant	0.24	mΩ
Inductance de l'aimant	2.43	μH
Puissance dissipée	0.101	kW
Energie stockée	730	J
	65	p en mm
	25	h en mm
	130	L en mm
	155	H en mm
Débit d'eau total	0.23	l/min
Débit dans chaque spire	0.23	l/min
vitesse de l'eau ( < 10m/s)	0.58	m/s
pression différentielle necess.	4.82	bar
Force septum /cond fond	1206.90	daN
Flèche max . septum (appui)	0.011	mm
moment flech.max. ( appui)	4.72	mm <sup>2</sup> daN
contrainte maxi <5 (appui)	3.15	daN/mm <sup>2</sup>
Masse culasse (sans poutre)	106	kg
longueur d'une spire	1.4883	m
section conduct. refroid.déduit	108	mm <sup>2</sup>
Section refroidissement	4.5	mm <sup>2</sup>





**Distribution:**

**M. Martini**

**J.P. Riunaud**

**C. Steinbach**

**Section PS/ PA/ Septa**